Multipath Parameter Estimation for Synthetic Aperture Sonar using the SAGE Algorithm

Ara Hyun[1], Woojae Seong[2]

[1]Department of Naval Architecture and Ocean Eng., Seoul National University, Seoul, Korea
[2]Research Institute of Marine Systems Eng., Seoul National University, Seoul, Korea

Abstract— *Operating synthetic aperture sonar (SAS) in shallow water environment can be challenging owing to multiply reflected signals interfering with the direct signal. We use the space-alternating generalized expectation maximization (SAGE) algorithm to estimate the multipath signal parameters. Specifically, we estimate the relative time delay of surface reflected signal to direct signal and the directions of arrivals of each signal. Using these estimates, we extract only the direct arrival signal which is used for SAS signal processing. Compared to using an adaptive beam-former, SAS system using the proposed algorithm shows better performance in terms of reducing multipath interference effects.*

Keywords—Multipath, parameter estimation, SAGE algorithm, synthetic aperture sonar.

I. INTRODUCTION

By coherently accumulating the received sonar signal as a sonar-equipped vehicle moves along its track, a long synthetic aperture reconstructs a high-resolution seafloor image. An interferometry, consisting of two or more vertically displaced arrays can produce improved bathymetry of the seafloor by offering precise bottom height [1], [2]. In shallow water environments, however, the bathymetry and image resolutions of the SAS system become poor due to the multipath interference effects. Reflected signal from the ocean surface is the dominant multipath interference; when we reconstruct image using SAS signal processing, the surface reflected signal creates a duplicate image of the target [3]. Since interferometry assumes that the phase of the received signal is determined by the line-of-sight distance from the reflector (target) to the sonar position, it is also detrimental to estimating the bathymetry due to surface reflected signals. Various algorithms reducing the multipath interference have been proposed to improve the performance of SAS systems [4]-[9]. In [4], [5], the belief propagation algorithm to reconstruct seafloor bathymetry was applied given *a priori* information on the likelihood of the height change between neighboring pixels. However, the belief propagation algorithm become computationally expensive for multipath environment. Adaptive beam-former approaches including MVDR (distortion-less processor) [10], [12] and MUSIC (multiple signal classification) [11], [12] have been used to mitigate multipath effects. These approaches spatially filter unwanted signals before application of SAS signal processing for reconstructing image and bathymetry. These approaches cannot be applied when time delays or directions of arrivals are similar. To overcome these limitations, a large vertical array is required. Alternatively, we can use a space alternating generalized expectation maximization (SAGE) algorithm, which is an extension of the expectation maximization (EM) algorithm [13], [14].

The SAGE algorithm extracts parameters such as complex amplitude, direction of arrival, time delay, and relative Doppler frequency according to paths from measurement data by iteratively approximating maximum likelihood estimate. The SAGE algorithm finds the parameters of each path sequentially whereas EM algorithm find the parameters of all paths simultaneously. The performance of the SAGE algorithm is better than that of classical techniques in terms of high-resolution ability and accuracy. The SAGE algorithm has been applied in radio mobile communication [15]. Recently, the SAGE algorithm has been applied to air and underwater navigation systems [15]-[20].

In this work, we use SAS signal processing with SAGE algorithm to suppress multipath interference effects in shallow-water environments. The robustness of the SAGE algorithm is examined with synthetic data consisting of direct and surface reflected signals. The signal model and assumption for the proposed algorithm are outlined and the method used to conduct the work and its implementations in the SAS system is described in Section 2. In Section 3, we show the results of applying the proposed algorithm to synthetic data and these results are compared to previous researches such as adaptive beam-former and EM algorithm. Finally, we conclude this work.

II. SAGE ALGORITHM

2.1 Signal Model

The SAS system in consideration is a horizontal uniform line array composed of N isotropic sensors (see Fig. 1), where the

spacing between sensors is Δ_x. Array transmitted signal is scattered by the target and these scattered signals are later measured at the array receiver.

When multiple signals impinge at the receiver, the received signal $y(t) \epsilon C^{1\times N}$ at a specific sonar position u can be expressed as:

$$\mathbf{y}(t,u) = \sum_{l=1}^{L} \mathbf{s}_l(t,u;\theta_l) + \mathbf{n}(t,u) \tag{1}$$

where $\mathbf{s}_l(t,u;\theta_l)$ is given by:

$$\begin{aligned} \mathbf{s}_l(t,u;\theta_l) &= \left[s_1(t,u;\theta_l),...,s_N(t,u;\theta_l)\right] \\ &= \mathbf{a}(\phi_l(t,u))\gamma_l(t,u)\, e^{j2\pi\nu_l(t,u)}\, p\left[t-\tau_l(t,u)\right] \end{aligned} \tag{2}$$

Here, $\mathbf{a}$ is the steering vector and $p(t)$ is the transmitted signal. Parameters $\boldsymbol{\theta}_l = [\gamma_l,\ \tau_l,\ \phi_l,\ \nu_l]$ are complex amplitude, time delay, direction of arrival, and relative Doppler frequency, respectively. We assume that the complex amplitudes of direct and ocean surface reflected paths are equal because of relatively little travel distance difference. Since direct and multipath signal are highly correlated, relative Doppler frequency is zero. Thus, we only need to estimate the time delays and direction of arrivals in this work. Here, $p(t)$ is the transmitted signal given by the following form:

$$p(t) = \begin{cases} \exp\left(j\beta t + j\alpha t^2\right), & 0 \le t \le T_p \\ 0, & \text{otherwise} \end{cases} \tag{3}$$

We use an LFM signal in order to obtain high range resolution. T_p is the pulse duration, α is the chirp rate and β is the minimum value of instantaneous frequency of (3) in the time interval when α and β are positive. Again, $a \epsilon C^{1\times N}$ is the steering vector of the array, which depends on ϕ_l : direction of arrival of the l th path contribution in the received signal. The steering vector at specific position becomes:

$$\mathbf{a}_l\left(\phi_l\right) = \left[1,\ ...,\ e^{jk\Delta_x n\cos\phi_l},\ ...,\ e^{jk\Delta_x (N-1)\cos\phi_l}\right], \quad 0 \le n \le N-1 \tag{4}$$

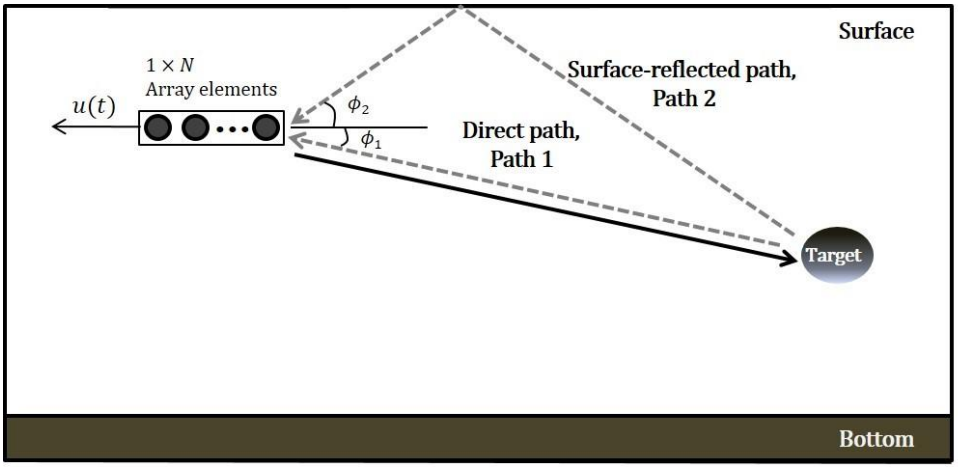

FIGURE 1: SCHEMATIC OF SAS GEOMETRY FOR A SHALLOW WATER ENVIRONMENT

In our signal model, we consider only the vertical direction multipath arrivals (see Fig. 1). In (1), the background noise $n(t,u) \epsilon C^{1\times N}$ assumes zero mean white Gaussian noise with known covariance. We also assume that the background noise at each element is spatially and temporally uncorrelated. The received signal at the specific position can be rewritten in matrix-vector notation as:

$$\begin{aligned}\mathbf{Y}(t) &= [\mathbf{Y}_1(t),\ldots,\mathbf{Y}(t)_N] \\ &= \mathbf{S}(t;\boldsymbol{\theta}) + \mathbf{N}(t) \\ &= \sum_{l=1}^{L}\mathbf{S}_l(t;\boldsymbol{\theta}_l) + \mathbf{N}(t)\end{aligned} \tag{5}$$

In (5), $\mathbf{S}_l(t;\theta_l)$ is the contribution of the l^{th} multipath signal.

2.2 SAGE Algorithm

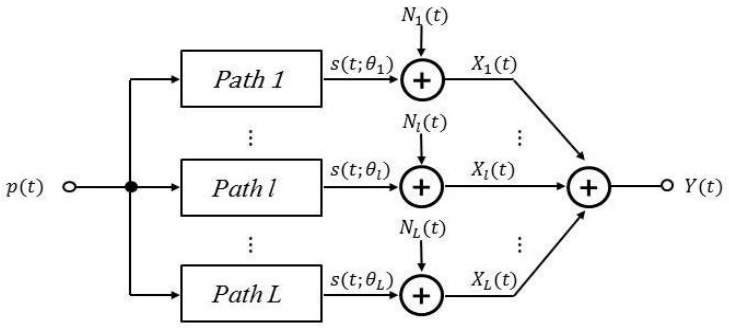

FIGURE 2: RELATION BETWEEN RECEIVED SIGNAL AND EACH PATH SIGNAL [15]

The SAGE algorithm is an advanced version of the EM algorithm, which is a well-known iterative method for estimating unknown parameters of a probability distribution function. The SAGE algorithm has a faster convergence rate as it updates the parameters sequentially in several small subsets. The $\mathbf{Y}$ in (5) is measurable and its measured signal is a stochastic function of signal from each path. By use of probability distribution of background noise, the corresponding maximum likelihood of parameters $\boldsymbol{\theta}_l = [\tau_l,\ \phi_l]$ would be [16]:

$$\mathrm{P}(\mathbf{Y};\theta) = \frac{1}{\left(\pi\sigma_n^{\,2}\right)^N}\exp\left(-\frac{\left\|\mathbf{Y}-\sum_{l=1}^{L}\mathbf{S}_l(t;\boldsymbol{\theta}_l)\right\|_F^2}{\sigma_n^{\,2}}\right) \tag{6}$$

where, N is the number of horizontal elements in an array and $\|\ \|_F^2$ denote the Frobenius norm of a matrix. The problem then is to estimate the parameters $\boldsymbol{\theta}_l = [\tau_l,\ \phi_l]$ of the l th multipath signal. We assume that background noise is 1×N dimensional vector of white Gaussian noise with known variance σ^2_n at the n th element.

The SAGE algorithm is based on the signal of each path X_l, which we call as hidden data, and received signal is a function of this hidden data (see Fig. 2). Since the hidden data cannot be measured, we should generate hidden data using the received signal and previous estimated parameters. The maximum likelihood estimate of $\boldsymbol{\theta}_l = [\tau_l,\ \phi_l]$ is the value for which the function of (6) is maximum; i.e., $\boldsymbol{\theta} = \arg\max_{\boldsymbol{\theta}}\{\mathrm{P}(\mathbf{Y};\boldsymbol{\theta})\}$.

The key idea of the SAGE algorithm is selection of hidden data composed of a subset for updating a subset of parameters at next cycle. Each iteration of SAGE algorithm consists of one or several cycles. An expectation step (E-step) and maximization step (M-step) are performed to estimate its subset and corresponding hidden data in cycle. All elements of parameters $\boldsymbol{\theta}$ split into $L\times p$ subsets of parameters as $\{\theta_c:\ 1\le c\le L\times p\}$, where p denotes the number of parameters at each path to be estimated for $X_l(t)$. Since our model considers time delay and direction of arrival, p is equal to two. Each subset associated c^{th} cycle, which corresponds to the hidden data, are sequentially updated with one iteration. After $L\times p$ cycles, all parameters of $\boldsymbol{\theta}$ are updated at each iteration. Each iteration retains the subset of parameters of other components fixed at previous values as $\boldsymbol{\theta}_c^i = \left(\theta_{c+1}^{i-1},\ \ldots,\ \theta_{L\times p}^{i-1},\ \theta_1^i,\ldots,\ \theta_{c-1}^i,\ \theta_c^i\right)$. For example, $\left(\theta_{c+1}^{i-1},\ \ldots,\ \theta_{L\times p}^{i-1},\ \theta_1^i,\ldots,\ \theta_{c-1}^i\right)$ are fixed at current state θ_c^{i}.

For estimation of parameters, let θ_c^i represent the estimate of the i th iteration and c th cycle and $\theta_1^i = \theta_{L\times p}^{i-1}$. The i th iteration of the SAGE algorithm consists of the E-steps and M-steps, as follows.
For $c = 1, \ldots, p \times L$, E-step calculate:

$$\hat{\mathbf{X}}_l(t;\hat{\boldsymbol{\theta}}_l) \triangleq E\left\{\mathbf{X}_l(t)\middle|\mathbf{Y}(t)\right\} \tag{7}$$

which is equivalent to computing:

$$\hat{\mathbf{X}}_l(t;\hat{\boldsymbol{\theta}}_l) = \mathbf{S}_l(t;\hat{\boldsymbol{\theta}}_l) + \left[\mathbf{Y} - \sum_{l=1}^{L}\mathbf{S}_l\left(t;\hat{\boldsymbol{\theta}}_l\right)\right] \tag{8}$$

where $\hat{\boldsymbol{\theta}}_l$ is estimated parameters of l th path at previous updating procedure.
M-step is updated by:

$$\begin{aligned}\theta_c^i &= (\hat{\tau})_{ML} = \arg\max_{\tau}\left\{\left|z\left(\tau,\hat{\phi};\hat{\mathbf{X}}_l\left(t;\hat{\theta}_l\right)\right)\right|\right\}\\ \theta_{c+1}^i &= \left(\hat{\phi}\right)_{ML} = \arg\max_{\phi}\left\{\left|z\left(\hat{\tau},\phi;\hat{\mathbf{X}}_l\left(t;\hat{\theta}_l\right)\right)\right|\right\}\end{aligned} \tag{9}$$

where

$$z\left(\tau,\phi;\hat{\mathbf{X}}_l\right) = \int p^H(t-\tau)a\left(\phi\right)^H\hat{\mathbf{X}}_l(t)\,dt \tag{10}$$

In (10), $p(t)$ is the transmitted signal, $a(\phi)$ is the steering vector, and H means Hermitian operator. The subset of parameters are updated by (9), where each parameter is updated sequentially. The E-step and M-step are performed iteratively until convergence is achieved. One SAGE iteration is required for estimation of all L signal parameters. Compared to the updating procedure of EM algorithm by (11), SAGE algorithm reduce 2D procedure of M-step into two separate 1D procedures, where each parameter is updated respectively by:

$$\hat{\boldsymbol{\theta}}_l = \left(\hat{\tau},\hat{\phi}\right)_{ML} = \arg\max_{[\tau,\phi]}\left\{\left|z\left(\tau,\phi;\hat{\mathbf{X}}_l\right)\right|\right\} \tag{11}$$

The SAGE algorithm can estimate parameters for all paths, but unfortunately not the number of multipath components L. Therefore, we assume that L is given.

2.3 Initialization of the SAGE algorithm

Initialization of the iterative method is a crucial problem. It is often advised to use randomly chosen initial values. To increase the convergence rate and estimate results as accurately as possible, the initialization of SAGE algorithm is considered as below.

To select the initial parameter, we find one index at the maximum correlation value between the transmitted and received signals:

$$(\hat{\tau}_0,\ \hat{\phi}_0) = \arg\max_{[\tau,\ \phi]}\left\{\left|\int_0^T y^H(t-\tau,\ \phi)\ p(t)\ dt\right|\right\} \tag{12}$$

where T is time duration of received signal. This procedure can reduce the number of iterations by offering a small candidate of estimating parameters. By choosing the initial parameter as above, the computational load of SAS processing can be reduced, which is considerable because the SAGE algorithm is performed at all sonar positions.

III. NUMERICAL EXPERIMENTS ON SAGE ALGORITHM PERFORMANCE

3.1 Numerical Experiments

In this numerical experiment, we examine the effect of multipath from the ocean surface on the reconstruction of target image and bathymetry using SAGE algorithm.

As stated previously, amplitudes of the direct path and reflected path from ocean surface are nearly equal because of relatively little travel distance difference. Then, we estimate the time delays and direction of arrival of two paths. Transmitted signal travels along two different paths (direct and surface reflected paths) but the two arrivals have high correlation. Under this condition, we cannot apply any of adaptive beam-formers or MUSIC to suppress multipath interference effects because of the highly correlated arrivals. Performance of MVDR also degrades when signal-to-noise ratio (SNR) is low. We will examine the robustness of the SAGE algorithm by comparing with the adaptive beam-formers.

This work focuses on an algorithm for one uniform line array. The transmitted signal is a LFM with a center frequency of 100 kHz and bandwidth of 20 kHz. The signal-to-noise ratio, which denotes the direct signal to background noise ratio, is 5 dB. Further details regarding simulation setup of SAS system are displayed in Table 1.

To demonstrate the capability of the SAGE algorithm, we conducted two different simulations (cases 1 and 2). Direct and surface reflected arrivals are well separated in case 1 whereas the signals are overlapped in case 2. Note that in case 2, direct signal cannot be extracted from the total received signal, thus making it more complicated and performance of adaptive beam-former should degrade. The signals for cases 1 and 2 are generated by using the pulse durations (T_p) and the SAS heights (h) given in Table 1.

TABLE 1
SPECIFICATIONS OF THE INSAS SIMULATIONS SYSTEM

Symbol	Definition	Value (case1/case2)	Unit
f_c	center frequency	100	kHz
f_0	baseband frequency	20	kHz
T_p	pulse duration	0.4/0.8	ms
σ_n	standard deviation	0.09	
SNR	signal to noise ratio at single element	5	dB
c	sound speed	1500	m/s
Δ_x	spacing between horizontal elements	0.0075	m
Nu	number of pings	810	
N	number of horizontal hydrophone elements	10	
L	synthetic aperture	20	m
H	shallow water depth	15	m
h	SAS height	5/3	m

3.2 Reconstruction of target image: Spherical rigid body

SAGE algorithm starts with initial value to generate the initial hidden data. Generally, initial values of all parameters are set to zero as $\boldsymbol{\theta} = [\tau_1,\ \phi_1,\ \tau_2,\ \phi_2] = [0,\ 0,\ 0,\ 0]$ [15]. In this work, we find one initial value by (12), which can reduce the number of iterations. As mentioned above, we determine the initial value by maximum amplitude of correlation between transmitted signal and received signal. Fig. 3 shows estimation of a possible direct signal, called hidden data at a certain iteration. The received signal is composed of two paths with time delays of 0.1334 s and 0.1373 s. Fig. 3(b) shows the estimated background noise; $\mathbf{Y} - \sum_{l=1}^{L} \mathbf{S}\left(\hat{\boldsymbol{\theta}}_l\right)$. At around 0.1334 s and 0.1373 s, the amplitude of the estimated background noise is higher than other amplitudes because the convergence condition for finding maximum likelihood estimate of background noise is not satisfied at this iteration. Thus, the estimated direct signal has subtle difference from the actual direct arrival in the received signal.

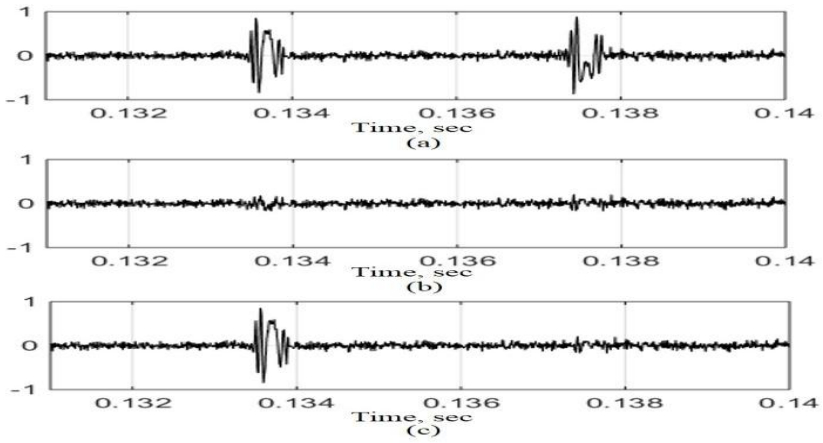

FIGURE 3: ESTIMATION OF POSSIBLE DIRECT SIGNAL
(A) RECEIVED SIGNAL, (B) ESTIMATED BACKGROUND NOISE, AND (C) ESTIMATED SIGNAL OF DIRECT SIGNAL

Using the signal of Fig. 3(c) with the estimated parameters at current iteration, we update new parameters by (9). And these parameters are used for generating hidden data again. After several repetitions, parameters eventually converge. Finally, signal of (8) with parameters sufficient to fulfill the condition for convergence is used to reconstruct the SAS image. The condition for convergence of the iterative procedure for estimating parameters should be fulfilled:

$$\ln\left(\mathrm{P}(\mathbf{Y};\hat{\theta})^{(i+1)}\right)-\ln\left(\mathrm{P}(\mathbf{Y};\hat{\theta})^{(i)}\right)\geq 0 \tag{13}$$

where, $\mathrm{P}(\mathbf{Y};\hat{\theta})^{(i)}$ is the likelihood function (6) of the estimated parameter at the i th iteration. $\hat{\theta}^{i+1}$ is an updated value that maximize the difference between log-likelihood functions at i th and $i+1$th iterations. So for each iteration, the log-likelihood function is non-decreasing because SAGE algorithm retains the monotonicity property of EM algorithm [13], [21]. The SAGE algorithm runs repeatedly as the SAS system proceeds with uniform speed at a constant depth. Since the number of parameters of each path and the number of paths are both two, this SAGE algorithm provides four converged parameters at each position u . Fig. 4 and Fig. 5 show converged time delay and direction of arrival from the SAGE algorithm for cases 1 and 2, respectively, as the SAS system traverses. Fig. 4 shows the results for a non-overlapping signal. Red line indicated the true parameter and blue is the estimated parameter using the SAGE algorithm. We can see that the estimated values are unbiased. Fig. 5 presents the results for an overlapping signal. Due to this circumstance, the difference in the time delay between the direct and surface-reflected signals is smaller than that in case 1, which suggests that the difference between directions of arrival is also smaller.

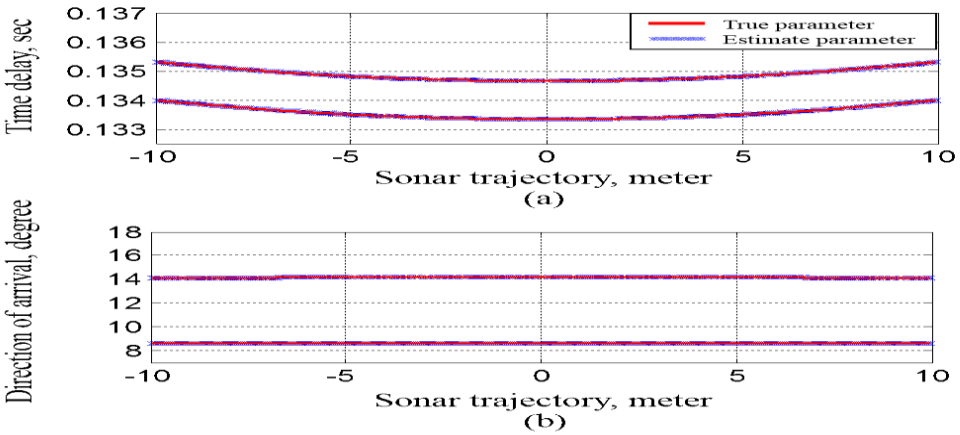

FIGURE 4: PARAMETER ESTIMATION IN CASE 1 (N=10)
(A) TIME DELAY AND (B) DIRECTION OF ARRIVAL

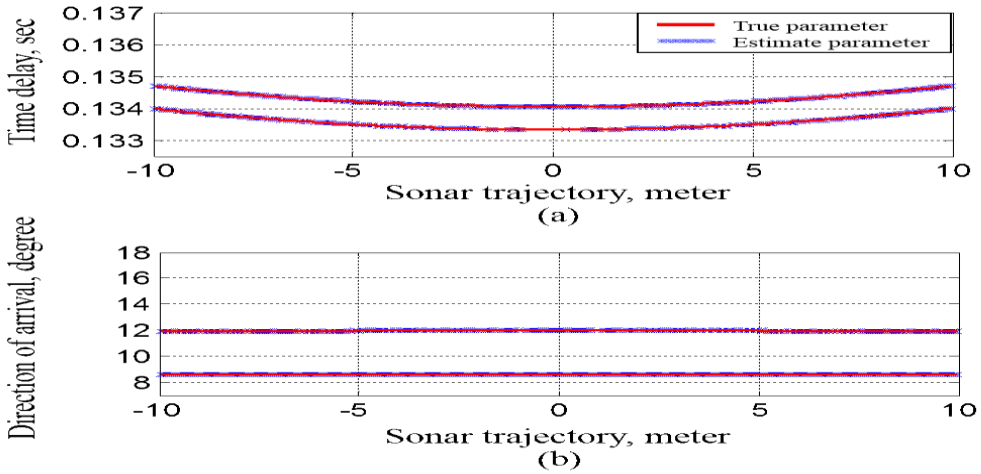

FIGURE 5: PARAMETER ESTIMATION IN CASE 2 (N=10)
(A) TIME DELAY AND (B) DIRECTION OF ARRIVAL

To show robustness of SAGE algorithm, we conducted broadband adaptive beam-former to estimate the directions of arrival in case 2. We add two more elements vertically above the first element of line array used for SAS image. The vertical spacing between elements is half wavelength of maximum frequency of transmitted signal. Fig. 6 shows the beam-former output using MVDR and MUSIC with 3 and 10 vertical elements. Because ϕ_2 is positive measured from array to surface and ϕ_1 is positive measured from array to bottom (see Fig. 1), the negative values in Fig. 6 are interpreted positive values in Figs. 4 and 5. From the result of MVDR in Fig.6, normalized beam-former output has one peak when we use only 3 vertical elements. However, two sources are separated well when we use 10 vertical elements. From this result, we need a large vertical array to distinguish each path. Nevertheless, even when we use 10 vertical elements, MUSIC algorithm cannot estimate the direction of arrival of each path because of high correlation between signals from each paths, in which case the ability of MUSIC degrades, due mainly to the fact that the spectral matrix is not full rank. Regarding direction of arrival, compared to the beam-former approaches in Fig. 6, the results in Fig. 4 and Fig. 5 demonstrate that the SAGE algorithm with single vertical line array facilitates precise estimation even in the complicated case 2.

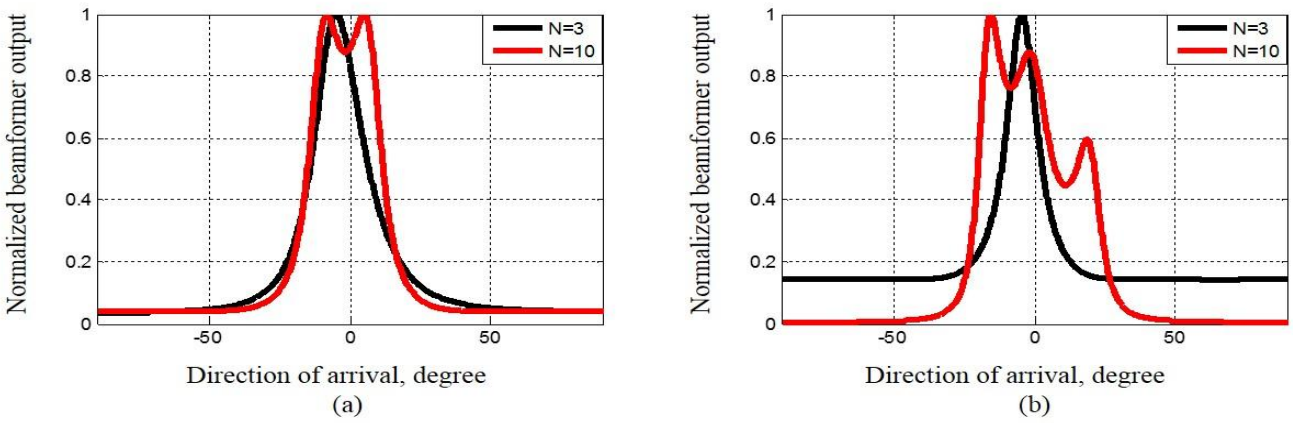

FIGURE 6: OUTPUT OF BEAMFORMER APPROACHES WITH 3 AND 10 VERTICAL ELEMENTS (CASE 2)
(A) MVDR AND (B) MUSIC

To examine the convergence rate related to computational complexity, we show the convergence of normalized likelihood according to iteration numbers of SAGE and EM algorithms (see (6)). Each curve represents the average of normalized likelihood over sonar trajectories. As expected, the SAGE algorithm shows faster convergence than the EM algorithm. EM algorithm converges at a relatively slow rate due to estimation of all parameters for all paths in parallel in a single iteration.

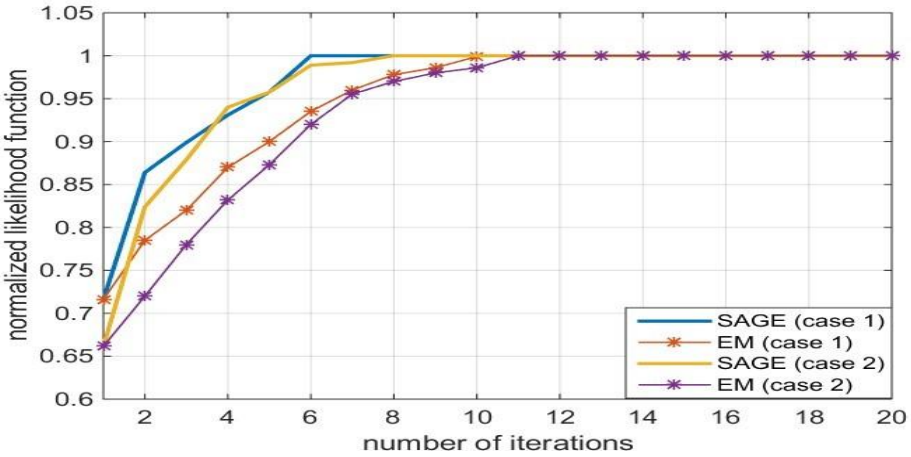

FIGURE 7: NORMALIZED LIKELIHOOD VERSUS ITERATIONS

The first step in SAS signal processing for operating in shallow water is to estimate the parameters of each path using the SAGE algorithm. With estimated parameters, we generated a direct path to reconstruct the target image and bathymetry. Fig. 8 shows the signals and reconstructed images of spherical rigid body shown in Fig. 1, before and after mitigating the multipath effect in the two cases by applying the SAGE algorithm; the first row is case 1 and the second row is case 2. (a) and (e) are received signals versus time and sonar trajectory in the presence of multipath signals with an SNR of 5dB. Background noise is reduced by averaging using 10 elements. From the reconstructed images in (b) and (f), we observe a duplicate image due to the multipath effect. Because of this duplicate image of the target, we cannot identify or localize the true target. Thus the duplicated image must be removed using the SAGE algorithm. (d) and (h) are the target images with signals of (c) and (g), where the multipath effect is mitigated using the SAGE algorithm. From (d) and (h), we can determine which curvature in (b) and (f) corresponds to the true target. The signals of (c) and (g) have errors in the background noise. In (c), the path is elongated at the end of the signal of the first path and the signal of the second path is not completely rejected. However, the error produced by the multipath in (b) is seen to become a point-like target as shown in (d), which would not cause any problem in distinguishing the real target image. The reconstructed images in (d) and (h) show that the target image can be distinguished using the estimated direct signal. Note that using this algorithm we can obtain the direct signal without beam steering using the estimated direction of arrival to remove multipath signals because images were reconstructed using the generated direct signal, known as the hidden data space.

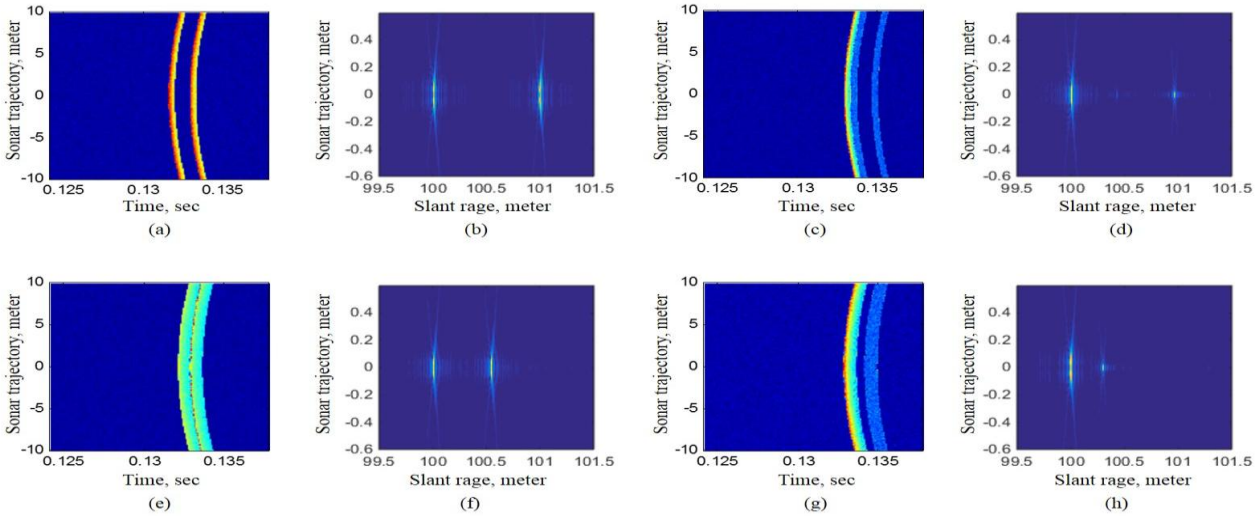

FIGURE 8: SYNTHETIC APERTURE SONAR SIGNAL AND RECONSTRUCTED IMAGE (A) RECEIVED SIGNAL IN CASE 1, (B) RECONSTRUCTED IMAGE OF (A), (C) MULTIPATH REDUCED SIGNAL OF (A), (D) RECONSTRUCTED IMAGE OF (C), (E) RECEIVED SIGNAL IN CASE 2, (F) RECONSTRUCTED IMAGE OF (E), (G) MULTIPATH REDUCED SIGNAL OF (E), AND (H) RECONSTRUCTED IMAGE OF (G)

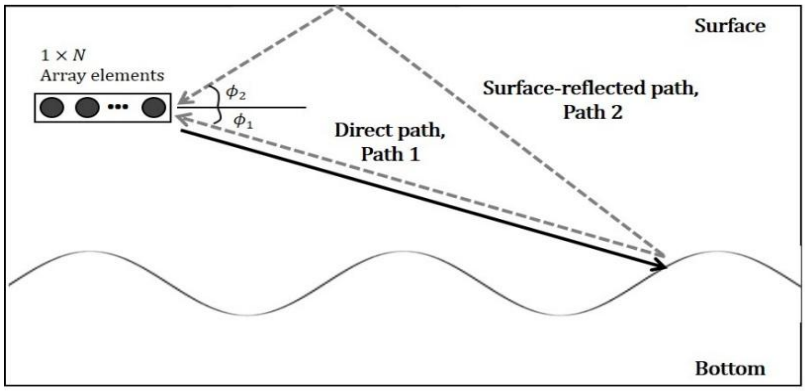

FIGURE 9: SCHEMATIC OF BATHYMETRY ESTIMATION

3.3 Bathymetry estimation

To demonstrate that it is possible to accurately estimate bathymetry using SAGE, we consider a sinusoidal seafloor with depth changing from 13.5m to 16.5m as shown in Fig. 9. SAGE results are compared to interferometry SAS (InSAS) results. Spacing between vertical arrays for In SAS is 0.03 m. To clarify the requirement for SAGE algorithm, we performed simulations in which the parameters were estimated both in presence and absence of multipath. Fig. 10 shows the bathymetry estimation result with direct path only. In this environment, the assumption for interferometry to extract the phase is fulfilled. The result of In SAS indicates a small estimation error since only two vertical arrays are used for bathymetry estimation. The simulation in Fig. 11 is identical to that in case 2 (overlapping direct and surface reflected signals), with the exception of SNR being 0 dB. The performance of estimation using interferometry degrades due to overlapping signals, which violates the assumption for interferometry. In Fig. 11, the values of 15 m and 20 m are midpoints between the crest and trough of direct and surface-reflected paths, respectively. The RMS error, used to evaluate interferometry performance, is 0.2 m and 3.4 m in Fig. 10 and Fig. 11, respectively. Compared to interferometry, the SAGE algorithm facilitates high-resolution bathymetry estimation irrespective of multipath.

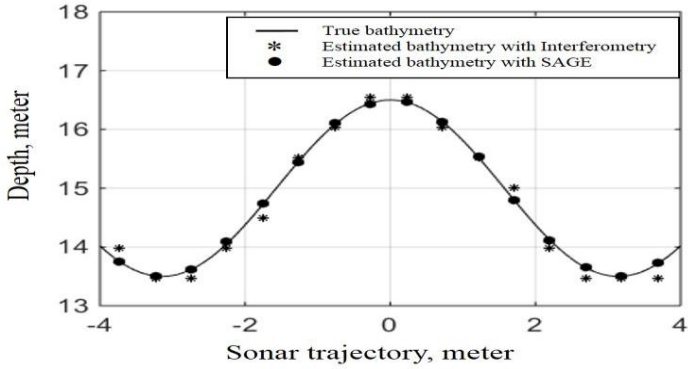

FIGURE 10: BATHYMETRY ESTIMATION IN A SINGLE-PATH ENVIRONMENT (SNR=0 DB)

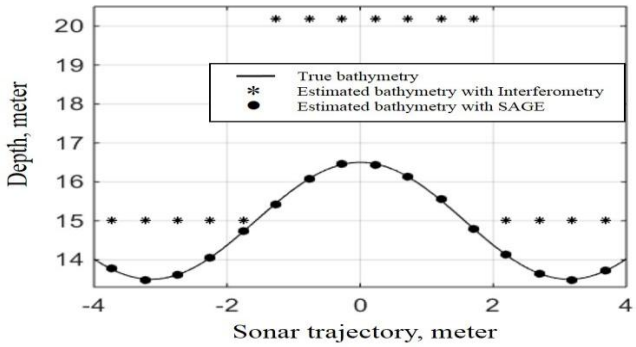

FIGURE 11: BATHYMETRY ESTIMATION IN A MULTIPATH ENVIRONMENT (CASE 2, SNR=0 DB)

3.4 Numerical experiment result

Iterative methods for reducing the multipath effects, such as SAGE, are performed at each sonar trajectory. Then, we consider the computational burden for operating SAS in a shallow-water environment. Fig. 12 shows the flow of multipath reduction processing for SAS in a shallow-water environment. In previous studies, the adaptive beam-former with a vertical array was used to estimate the most likely delay, $\hat{\tau}$,which is used to determine bathymetry with baseline and slant range. SAS image reconstruction is implemented using a direct signal retrieved by beam selection, which forms vertical beams to determine the most likely direction of arrival and time delay of the direct signal.

Unlike adaptive beam-formers, the SAGE algorithm with one element or horizontal array can estimate the direction of arrival $\hat{\phi}$, time delay $\hat{\tau}$, and direct signal $\hat{X}_l$ prior to SAS signal processing. Because the direct signal can be obtained directly, this signal is used to reconstruct the SAS image. Also, bathymetry estimation is conducted using the estimated parameters. Although iterations are needed to estimate the parameters at each sonar trajectory, this process does not require beam selection to retrieve the direct signal $\hat{X}_l$ as in previous approaches.

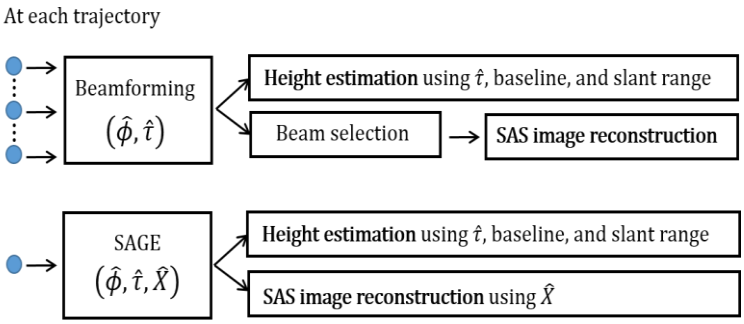

FIGURE 12: MULTIPATH REDUCTION PROCESSING FOR THE SAS SYSTEM IN SHALLOW WATER

IV. CONCLUSION

This work has dealt with the multipath problem for SAS in shallow-water environments. To achieve reliable SAS performance, we estimated the parameters of direct and multipath signals.

Based upon numerical experiments using synthetic data, the SAGE algorithm showed better performance than adaptive beam-former approaches in terms of reducing the multipath effect. With horizontal elements, it was possible to precisely estimate the parameters of direct and surface reflected signals. In contrast to earlier findings, a high resolution of parameters could be obtained using a small number of iterations.

In this work, we also conducted simulations using overlapping and non-overlapping case of direct and multiply reflected signals to verify the ability of SAGE algorithm. We compared bathymetry estimation of the SAGE algorithm with that of interferometry. The results demonstrate that SAGE algorithm can obtain high-resolution bathymetry in shallow-water environments regardless of the characteristics of the received signal. As explained above, unlike interferometry, the SAGE algorithm in a multipath environment does not require a vertical array to obtain high-resolution bathymetry.

This work shows that the proposed algorithm is capable of providing high-resolution parameters to generate direct signals for an SAS system. Because multipath effects need not be mitigated using two or more vertical arrays, the SAS system employing SAGE algorithm does not need to be large, heavy, power-hungry and costly.

REFERENCES

[1] X. Lurton, "Swath bathymetry using phase difference: theoretical analysis of acoustical measurement precision," IEEE Oceanic Engineering, vol. 25, no. 3, pp. 351-363, July 2000.

[2] H. D. Griffiths, "Interferometric synthetic aperture sonar for high-resolution 3D mapping of the seabed," in Proc. Radar, Sonar and Navigation, IEE proceedings, April 1997.

[3] B. J. Davis, P. T. Gough, and B. R. Hunt, "Modeling surface multipath effects in synthetic aperture sonar," IEEE Oceanic Engineering, vol. 34, no. 3, pp. 239-249, July 2009.

[4] P. J. Barclay, C. J. Forne, M. P. Hayes, and P. T. Gough "Reconstructing seafloor bathymetry with a multichannel broadband InSAS using belief propagation," in Proc. Oceans 2003, September 2003.

[5] M. Hayes and P. Barclay, "The effects of multipath on a bathymetric synthetic aperture sonar using belief propagation," in Proc. Image and Vision Computing, New Zealand, November 2003.

[6] M. Hayes, "Multipath reduction with a three elements interferometric synthetic aperture sonar," in Proc. European Conf. Underwater Acoustic (ECUA), July 2004.

[7] A. E. A. Blomberg and M. Hayes, "Multipath reduction for bathymetry using adaptive beamforming," in Proc. OCEANS 2010, May 2010.

[8] Q. Chen, W. Xu, X. Pan, and J. Li, "Wideband multipath rejection for shallow water synthetic aperture sonar imaging," IET Radar, Sonar & Navigation, vol. 3, no. 6, pp. 620-629, December 2009.

[9] W. Xu, Q. Chen, J. Li, F. Sun, and X. Pan, "Results of a three-row synthetic aperture sonar for multipath rejection," in Proc. Oceans 2010, September 2010.

[10] D. H. Johnson, "The application of spectral estimation methods to bearing estimation problems," in Proc. IEEE, vol. 70, no. 9, pp. 1018-1028, September 1982.

[11] R. O. Schmidt, "Multiple emitter location and signal parameter estimation," IEEE Transactions on Antennas and Propagation, vol. 34, no. 3, pp. 276-280, March 1986.

[12] H. Cox, R. Zeskind, and M. Owen, "Robust adaptive beamforming," IEEE Transactions on Acoustics, Speech and Signal Processing, vol. 35, no. 10, pp. 1365-1376, October 1987.

[13] J. A. Fessler and A. O. Hero, "Space-alternating generalized expectation-maximization algorithm," IEEE Transaction on Signal Processing, vol. 42, no. 10, pp. 2664-2677, October 1994.

[14] P. J. Chung and J. F. B Böhme, "Comparative convergence analysis of EM and SAGE algorithms in DOA estimation," IEEE Transaction on Signal Processing, vol. 49, no. 12, pp. 2940-2949, December 2002.

[15] B. H. Fleury, M. Tschudin, R. Heddergott, D. Dahlhaus, and K. Pederson, "Channel parameter estimation in mobile radio environments using the SAGE algorithm," IEEE Journal on Selected Areas in Communications, vol. 17, no. 3, pp. 434-450, March 1999.

[16] F. Antreich, J. Nossek, and W. Utschick, "Maximum likelihood delay estimation in a navigation receiver for aeronautical applications," Aerospace Science and Technology, vol. 12, no. 3, pp. 256-267, April 2008.

[17] S. Rougerie, G, Carrie, F. Vincent, L. Ries, and M. Monnerat, "A new multipath mitigation method for GNSS receiver based on an antenna array," International Journal of Navigation and Observation, March 2012.

[18] S. Rougerie, A. Konovaltsev, M. Cuntz, G. Carrie, L. Ries, F. Vincent, and R. Pascaud, "Comparison of SAGE and classical multi-antenna algorithms for multipath mitigation in real-world environment," in Satellite Navigation Technologies and European Workshop on GNSS Signals and Signal Processing (NAVITEC), December 2010.

[19] S. Mota, M. Garcia, A. Rocha, and F. Perez-Fontan, "Estimation of the radio channel parameters using the SAGE algorithm," Radioengineering, vol. 19, no. 4, pp. 695-702, December 2010.

[20] K. Hausmair, K. Witrisal, P. Meissner, C. Steiner, and G. Kail, "SAGE algorithm for UWB channel parameter estimation," in COST 2100 Management Committee Meeting, February 2010.

[21] G. J. McLachlan and T. Krishnan, The EM algorithm and extensions, John Wiley & Sons, 2nd ed., vol. 382, New Jersey, USA, 2008.